A methodology to conduct wind damage field surveys for high impact weather events of convective origin

Oriol Rodríguez[1], Joan Bech[1], Juan de Dios Soriano[2], Delia Gutiérrez[2], and Salvador Castán[3]

[1]Department of Applied Physics - Meteorology, University of Barcelona, Barcelona, 08028, Spain
[2]Agencia Estatal de Meteorología, Sevilla, 41092, Spain
[3]Agencia Pericial, Cornellà de Llobregat, 08940, Spain

Correspondence: Oriol Rodríguez (orodriguez@meteo.ub.edu)

Abstract. Post-event damage assessments are of paramount importance to document the effects of high-impact weather events such as floods or strong wind events. Moreover, evaluating the damage and characterizing its extension and intensity can be essential for further analysis such as completing a diagnostic meteorological case study. This paper presents a methodology to perform field surveys of damage caused by strong winds of convective origin, i.e. tornado, downburst and straight-line winds. It is based on previous studies and also on 136 fieldworks performed by the authors in Spain from 2004 to 2018. The methodology includes the systematic collection of pictures and records of damage on man-made structures and on vegetation, as well as collection of available Automatic Weather Station data, witness reports and images of the phenomenon, such as funnel cloud pictures. To synthesize the data recorded in the damage field survey, three final deliverables are proposed: (i). A standardised summary of the fieldwork; (ii). A table consisting of detailed geolocated information about each damage point and other relevant data, and (iii). A map or a KML file containing the previous information ready for graphical display and further analysis. This methodology has been applied by the authors in the past, sometimes only a few hours after the event occurrence and, in many occasions, when the type of convective phenomenon (e.g. tornado, downburst) was uncertain. In those uncertain cases, the information resulting from this methodology contributed effectively to discern the phenomenon type thanks to the damage patterns analysis, particularly if no witness reports were available. The application of systematic methodologies as the one presented here is necessary in order to build homogeneous and robust databases of severe weather cases and high impact weather events.

1 Introduction

Meteorological phenomena associated with strong surface winds from convective origin, which include tornadoes, downbursts and straight-line winds, can cause important disruption to socio-economic activity, including injuries or even fatal victims despite their local character compared to larger scale mid-latitude synoptic windstorms or tropical storms. For example, from 1950 to 2015, tornadoes in Europe caused 4,462 injuries, 316 fatalities and economic losses of at least €1 billion (Antonescu et al., 2016, 2017). Due to their economic and social impact, a large number of previous studies have been devoted to study these phenomena both from the point of view of their consequences (as in Strader et al., 2015) or specifically from a meteorological point of view (see for example Taszarek et al., 2017; Miller and Mote, 2018 or Rodríguez and Bech, 2018).

Analysing damage using the information gathered during a strong-convective wind survey assessment can be essential to determine which phenomenon took place (Bunting and Smith, 1993; Doswell, 2003), for instance, estimating the wind field from the fallen trees direction (Hall and Brewer, 1959; Holland et al., 2006; Bech et al., 2009; Beck et al., 2010; Rhee and Lombardo, 2018). When these phenomena affect a sparsely populated area, or they occur in a low visibility environment due to night darkness or intense precipitation, there is usually a lack of direct witnesses and recorded images. In that case, the task of assessing the damage intensity and discriminating if it was caused by a tornado, a downburst or another type of convective winds can be very challenging.

Despite the recent progress on assessing wind damage using high resolution radar observations (see Wurman et al., 2013 or Wakimoto et al., 2018), the systematic elaboration of post-event forensic field surveys is still the standard way to evaluate the damage caused by these meteorological phenomena (Marshall, 2002; Marshall, 2012; Zanini et al., 2017), similarly to field surveys of hailstorms (Farnell et al., 2009) or floods (Molinari et al., 2014; Li et al., 2018). A detailed damage analysis from a strong-convective wind event allows to characterize it in detail (see for example Burgess et al., 2014; Meng and Yao, 2014; Bech et al., 2015), estimating damage path length and width, and wind maximum intensity using a wind damage scale such as the Fujita scale (Fujita, 1981) or the Enhanced Fujita scale (EF-scale, WSEC, 2006).

Moreover, in order to increase our understanding of the meteorological processes involved in the genesis of severe weather events, if enough evidence are available, it is important that field surveys can discriminate if the phenomenon was a tornado, a downburst or straight-line winds so this information can be added to natural hazards databases such as the USA Storm Prediction Center Severe Weather Database (Verbout et al., 2006) or the European Severe Weather Database (Dotzek et al., 2009). This motivation, together with the fact that high-densely populated coastal areas are among the regions most affected by tornadoes in the area of study (Bech et al., 2007, 2011; Mateo et al., 2009; Gayà et al., 2011; Sánchez-Laulhé, 2013; Riesco et al., 2015) and also in other Mediterranean countries (Matsangouras et al., 2014; Miglietta and Matsangouras, 2018; Renko et al., 2018), contribute to the development and application of this study.

The objective of this paper is to propose a methodology to conduct wind-field post-event damage surveys of convective-driven events systematically. It can contribute to improve the detection, mapping and characterization of wind damage in a homogeneous way, which is important to better describe specific meteorological phenomena, with the particularities associated with damage from convective local storms. Therefore, the main goal of the proposed methodology is to represent the damage scenario to study strong-convective winds phenomena from a meteorological point of view, contributing to the creation and maintenance of homogeneous databases of severe weather events that discriminate among tornadoes, downbursts and other convective winds. Additionally, the determination of the strong-convective wind phenomena causing damage might not be only for a meteorological interest. For instance, current legal regulations in Spain set different insurance compensations for tornadic and non-tornadic cases (De Groeve et al., 2014): in order to be compensated, the latter require a wind speed threshold exceedance while the former do not, so forensic studies clarifying this aspect are regularly employed to decide upon insurance compensation.

Moreover, as it is mentioned in De Groeve et al., (2013, 2014), data gathered in a fieldwork may be also useful to further analyse the exposition and vulnerability of damaged man-made structures, and to study the impact of strong convective wind phenomena in an area. In addition, all this information can also be used to enhance or compliment wind intensity rating scales, as presented, for example, in Mahieu and Wesolek (2016).

The methodology presented here is based on previous studies (Bunting and Smith, 1993; Marshall, 2002; Doswell, 2003; Gayà, 2018; Holzer et al., 2018) and also on 136 fieldworks performed in Spain from 2004 to 2018 by the authors (Fig. 1), especially in Catalonia and Western Andalusia, and can be readily applied elsewhere. The proposal includes the systematic collection of pictures and records of damage on man-made structures and on vegetation, as well as Automatic Weather Station (AWS) data available, witness reports and images of the phenomenon together with their location and orientation. Three final deliverables are suggested to synthesize the data recorded: (i). A summary of the fieldwork; (ii). A table consisting of detailed geolocated information, iii). A map or a KML (Keyhole Markup Language) file containing the previous information ready for graphical display and further analysis.

The rest of the article is organized as follows. Section 2 describes in detail the field survey methodology proposed. In Sect. 3 specific limitations of the methodology are discussed and criteria for discriminating between tornado and other convective wind damage on forest areas are given. Section 4 presents a summary and final conclusions. As Supplementary material, an example of deliverables (text summary, table and KML file) of a damage survey of a recent tornadic event in Catalonia (see Fig. 1) is provided with the aim to better illustrate the methodology proposed and to facilitate its application.

2 METHODOLOGY

As stated in previous related work, the basic idea behind wind damage surveys is collecting as much information as possible about the relevant consequences of the convective phenomenon, geolocating properly the damage (Bunting and Smith, 1993; Doswell, 2003). The methodology to carry out damage surveys must be efficient, making possible to visit the affected area in the shortest possible time. It must be also easily reproducible and its results should be accurate. Geolocating damage using pictures or videos recorded with smartphones, or cameras with a Global Navigation Satellite System such as GPS fulfils these conditions (Edwards et al., 2013). Nevertheless, as it happens with other types of damage assessments, there are inherent uncertainties that should be taken into account when analysing field data (Beven et al., 2018), like possible GPS location errors or ambiguous application of intensity-rating assessments due to EF-scale limitations, which are discussed on Sect. 3.

Smartphone or cameras with GPS image geolocation and orientation (azimuth pointing) capabilities provide essential data to carry out a fieldwork in order to geolocate damage, as mentioned previously. Moreover, a compass and a tape measure are also highly recommended, as well as a hand counter device to count uprooted or snapped trees and, ideally, a portable suitcase balance to weigh wind-borne debris. As it is indicated in Bunting and Smith (1993) and Gayà (2018), water, food, comfortable footwear, rain jacket, spare clothes and a mobile phone spare battery are recommended, because affected areas may be far away from inhabited locations. As the affected area can require surveyor displacements longer than a few kilometres, a well-equipped, preferably all terrain, car is necessary to save time between points-of-damage analysis. Nevertheless, difficult access areas may be found along the track, because of muddy roads and fallen trees or simply because of the absence of roads. Especially in these cases, and also to study in detail damaged areas, walking is the other basic way to perform the field survey.

Despite this may not be always feasible, it would be ideal that the damage survey team was multidisciplinary, being formed by meteorologists, insurance inspectors, forestry engineers and architects experienced on damage assessments, at least familiar with damage reporting systems such as the EF-scale. This would facilitate an accurate and detailed analysis of the damage and the phenomenon intensity.

The proposed methodology is organized in three stages – see the flowchart in Fig. 2 for a schematic overview. The first step includes pre in-situ damage survey tasks, preparing the actual visit of the damaged area. Secondly, the in-situ fieldwork tasks, which include direct gathering of man-made structure and vegetation damage information, and also direct witness experiences. Finally, post in-situ damage assessment tasks, which involve ordering and organising all the information collected into three deliverables (a damage survey summary, a geolocated information table and a data location map).

2.1 PRE IN-SITU SURVEY TASKS

In order to properly prepare the damage survey, a number of previous tasks must be performed. One of them is planning the route of the in-situ survey. As mentioned in Holzer et al. (2018) it is strongly recommended to start damage surveys as soon as possible, especially if urban areas have been affected. Emergency and clearing services may start repairing tasks only a few hours after the event, which can alter the quality and quantity of possible information available during the survey – see for example Fig. 3. Therefore, and also to optimize time and resources, a detailed planning is necessary to carry out the field survey.

Firstly, preliminary information should be gathered about damage location and images available on the media and social networks, which are the main providers of strong-convective winds reports nowadays (Hyvärinen and Saltikoff, 2010; Knox et al., 2013; Kryvasheyeu et al., 2016). Citizen science collaborative platforms covering different geographical domains such as the European Severe Weather Database (ESWD, Dotzek et al., 2009), the severe weather database from the Spanish Meteorological Agency (SINOBAS, Gutiérrez et al., 2015) or the meteorological spotters platform from the Meteorological Service of Catalonia (XOM, Ripoll et al., 2016), are also examples of valuable sources of tornado and downburst reports. These reports may contain information about damage and/or a developed funnel cloud. Funnel clouds (see Fig. 4) are a typical feature of tornadic storms though sometimes may form without developing a tornado. When damage reports are available (Case 1 in Fig. 2), their location should be found by contacting with their authors and/or using GIS cartography, proceeding as the case described in Holzer et al. (2018). Applications such as Google Street View can be very useful to carry out this task.

Nevertheless, if no damage reports but only developed funnel cloud reports are available (Case 2 in Fig. 2) then their location and orientation should be estimated from meteorological observations such as weather radar or lightning data and GIS cartography. Then a possibly affected area can be preliminarily identified where the damage survey should be carried out. The more details about funnel clouds (different pictures or videos from different perspectives) are available, the more precise can be the location of the preliminary damage area. However, at this stage it has to be kept in mind the possibility that the funnel cloud may have not produced damage, either due to the lack of man-made structures or trees in the area intercepted by the tornado, or because the strong rotation associated to the funnel cloud actually did not touch down. This possibility will be verified during the in-situ survey tasks.

Contacting emergency services and local authorities can also provide valuable information, as they may record detailed damage data, especially if an urban area is affected. This kind of information may be crucial because clearing services might start arrangement tasks before in-situ visit is started. Occasionally, they may take damage aerial recordings, which can be very useful to complement the damage survey assessment.

Analysis of satellite and weather radar imagery is required to estimate the approximate timing of the event and the movement of the convective parent storm that may have produced the phenomenon. That information should be considered in order to extend the initial evidences of a preliminary damage path (looking for possible initial and ending damage path points) and also to assess the consistence of reports by direct or indirect eyewitnesses.

On the other hand, existing automatic weather stations in the area of interest can play an important role to determine the phenomenon type, the timing of the event and also to estimate the wind strength (Letchford, 2002; Karstens et al., 2010). Therefore, it is strongly recommended to search and locate all weather stations in the area of study, requesting the data with the maximum temporal resolution (see Fig. 5 as an example), and performing basic quality control (time consistency and comparison with official observations) before use.

Another important task before starting the actual in-situ damage assessment is to check the wind climatology of the studied area, particularly in windy regions (either because of the orography or the prevailing synoptic conditions; Feuerstein et al., 2011). In that case, man-made structures and vegetation are adapted to resist strong winds –sometimes from specific directions– and wind speed damage thresholds may be higher than in non-windy regions. Therefore, if a weak tornado or microburst affects a region usually influenced by strong winds, it is possible that little or no damage is found. Similarly, the application of an intensity damage scale in very windy regions may require some adjustments -i.e. relaxing the damage thresholds- as it is also discussed in Feuerstein et al. (2011).

In some occasions, the studied area may have been affected recently by another damaging windstorm or by a heavy snowfall which may have produced widespread damage in forests – for example due to wet snow as described in Bech et al. (2013) and Llasat et al. (2014). In those cases, the data collection process may be hampered by possible overlapping damage and, consequently, great care must be taken to identify the most recent one and to avoid mixing recent with previous damage. A possible way to mitigate this problem is asking locals about previous events and paying attention to the dryness from affected trees and broken branches, which can indicate if forest damage is recent or not.

2.2 IN-SITU SURVEY TASKS

To avoid alterations on the damage scenario due to clearing services, the fieldwork should preferably start on the most resilient areas, i.e. where socio-economical activity is more intense and are more likely to be recovered quickly. The proposed priority order is to visit urban areas first, then damaged electrical transmission or telecommunication lines, industrial parks and urban parks and, finally, forest and other surrounding areas (see Fig. 2).

As a general principle, the highest possible number of relevant damaged elements should be analysed on the affected area, both man-made structures and natural (vegetation) elements. Interviews to eye-witnesses, which can provide key information about the event and also other damaged areas, are also very important. The next subsections cover these aspects in more detail.

2.2.1 MAN-MADE STRUCTURES DAMAGE ASSESSMENT

Man-made structural damage analysis is essential to estimate the phenomenon wind intensity, for example using the EF-scale. As explained in WSEC (2006), the Enhanced Fujita scale considers several Degrees of Damage (DoD) from a total of 23 Damage Indicators (DI) related to constructions and 3 DI from other man-made structures that can be used to determine the 3-seconds wind gust speed associated to these damages.

In the present methodology it is proposed to geolocate every damaged structure on the affected area, whose coordinates (latitude and longitude) can be obtained from the GPS receiver of the photo camera (with a typical precision of $\pm 1 \cdot 10^{-4}$ deg., see Table 1). It is also convenient to take one or more pictures from each damaged element, both general and detailed views that may be of interest to evaluate the damage intensity (Marshall, 2012; Roueche and Prevatt, 2013). These photos should also be used during the post in-situ damage survey analysis to study which type of strong convective wind phenomenon caused the damage.

Moreover, for each affected man-made structure, the pair of DI-DoD data values should be provided by using an intensity-rating scale as the EF-scale, as proposed in Burgess et al. (2014) and Holzer et al. (2018). This task can be carried out during the damage survey, but it is recommended to perform it during the post in-situ damage assessment analysis. The main reason is to optimize the time and sources devoted to the in-situ survey. In case that no DI could be associated to the damaged element, it should be explicitly shown as ‘unrated’.

It is highly recommendable to check the maintenance status of the damaged man-made structures to avoid a biased intensity determination. Previous weaknesses or deficiencies on construction can make structures more vulnerable to strong winds and so a higher Degree of Damage might be caused for an expected wind speed. For example, if an absence of anchors or the presence of rust on metal beams from a roof are observed, this should be explicitly documented by pictures and a brief description to be taken into account when a damage-rating scale is applied, as already proposed by Fujita (1992).

The estimated trajectory and distance covered by wind-borne debris, as well as its size and weight, may also provide valuable information to estimate wind velocity associated to the studied phenomenon (Knox et al., 2013). Therefore, it is recommended to measure the dragged or flying distance and direction of objects of interest, if origin and final locations are known, using a tape measure or GIS tools (Table 1). It is also interesting to document its weight, either estimated consulting bibliography or measuring it by a portable balance in case of small objects (the relative error should be less than 10 %).

2.2.2 FOREST DAMAGE ASSESSMENT

As explained in Sect. 1 the maximum wind field (direction and intensity) associated with a strong-convective wind event can be approximately derived from the fallen trees pattern. Therefore, if a substantial number of trees are damaged to produce a clear damage pattern, a detailed forest damage study is recommended. As described in detail in Sect. 3.3, if fallen trees present a convergence and rotational pattern along a linear path, it is likely it was caused by a tornado, whereas if divergent damage patterns, mostly nonlinear, are observed, the most likely cause is a downburst. This analysis is especially interesting for those cases where there is no image nor direct witness of the phenomenon to determine the damage origin.

The forest damage survey should be carried out similarly to the man-made structure damage assessment, taking pictures of every relevant damaged vegetation element and registering its location (latitude and longitude). In case of uprooted trees, the fall direction should be measured using a compass with 5 deg. of precision (see Table 1). However, it should be noted that fall tree directions may be influenced by local factors and not be representative of the wind direction. For example, trees falling on a steep slope terrain (favouring one fall direction over others) or the presence of another nearby tree falling first can alter the tree direction with respect to the dominant wind. Therefore, in these cases it is recommendable not to consider the data. In case of snapped trees, trunk diameters should be measured with a measuring tape (with a resolution of 5 cm; Table 1). This data can help in the damage-rating task. However, as there may be a large number of damaged trees in a forest area, it is advisable to collect data from the most representative ones (for example, where tree fall direction changes or converges, probably indicating the effects of air rotation; or where damage is most significant, and surrounding damaged trees to delimitate the damage swath width).

Damage in forest areas can be also useful to evaluate the phenomenon intensity. The EF-scale (WSEC, 2006) describes different wind velocity ranges for five Degrees of Damage (DoD), namely small limbs broken, large branches broken, trees uprooted, trunks snapped and trees debarked with only stubs of largest branches remaining. As wind effect on trees also depends on the tree species (Foster, 1988; see for example Fig. 6a), the EF-scale also distinguishes between softwood and hardwood trees. Thus, DI-DoD pairs for each analysed vegetation element should be provided.

Moreover, soil characteristics can affect tree stability; in case of very moist soil, or thin soil over rocky subsoil, trees can be uprooted more easily, as it is illustrated in Fig. 6b. Trees health can also alter the resistance to strong winds. As it is done for man-made structures, these debilities must be stated in the report. In order to refine intensity-rating tasks in forests, it is recommended to calculate the ratio of affected trees in 50 m x 50 m areas if possible; it can be related to the EF-scale, according to Godfrey and Peterson (2017). High-resolution aerial imagery (i.e. from helicopter or drone) can be very useful to carry out this task. This analysis is especially interesting in the most severely affected forest area of the damage swath.

Most tornado damage paths are less than 5 km long; for example, in Spain only 25 % of tornado identified tracks are longer than 5 km (Gayà, 2018). Therefore, a detailed forest damage analysis is usually possible. However, in cases where damage is widespread, a complete detailed analysis may be not be feasible. To solve that, it is recommended to study discontinuous segments every 250-500 metres along the expected damage path. This allows estimating the path width and looking for the damage continuity. In addition, as previously commented, aerial images can enhance the forest damage analysis, especially in case of large damage swaths and difficult access areas (Karstens et al., 2013). Alternative approaches to surveys over widespread forest damaged areas are satellite image processing, as recently reported by Chernokulsky and Shikhov (2014), Shikhov and Chernokulsky (2018) and Shikhov et al. (2019).

2.2.3 WITNESS ENQUIRIES

Direct witnesses, if available, are an important source of information often essential to determine which type of strong convective wind phenomenon occurred. Witnesses experience of the event and their possible knowledge of other witnesses in nearby damaged locations can be very useful to complement a damage survey. In Bunting and Smith (1993) and Gayà (2018) it is noted that a direct witness may have been emotionally or physically affected by the phenomenon (for example private property damaged or close persons injured) so it is necessary to be respectful and careful during the enquiry.

It is important to let witnesses explain with their own words their experience of the event, and interviewers should avoid using key words such as tornado, downburst or gust front, particularly in those cases when the phenomenon type is not known yet. The terms used by the witness may provide useful clues about what happened. In addition, it is necessary to consider that previous media reports can alter the explanation of witnesses; for example, if the event has already been described as a tornado in the media, even if evidences of rotation are not found in the damaged area, people will probably say that a tornado has occurred.

A brief and concise inquiry, with specific questions but allowing open answers that may unveil relevant information, is proposed. Recommended questions are shown in Table 2. In some occasions, a direct witness may have taken photos or videos of the phenomenon that can be helpful for the study. When available, they should be treated as described in Sect. 2.1.

2.3 POST IN-SITU SURVEY TASKS AND DELIVERABLES

When the in-situ damage survey is completed, the event analysis should be complemented using meteorological remote-sensing data, which now can be compared with the records obtained in the survey. The information collected by direct witnesses, pictures, and videos usually allow to restrict the event occurrence to a temporal window of about 15 minutes to 2 hours. Satellite imagery and data from Doppler radar, lightning detection systems and AWS (particularly if located within or close to the damage swath) from the period of interest can provide the necessary information to identify the convective structure responsible of the damage. In particular, the starting and ending time of the event can be estimated by checking the time when the convective structure passed over the initial and the final point of the damage swath, respectively, with an error typically less than 5 minutes. It is recommended to perform this comparison with Doppler radar observations, if available, with data in original polar coordinates keeping the highest spatial resolution (see for example Bech et al., 2009; 2011; 2015). In some cases, it is even possible to estimate the mean translational velocity and direction of the convective cell, knowing the distances between initial and final damage path and the starting and ending time of the event. This can be very useful to fit theoretical surface wind vortex models to be compared with the observed damage patterns over forest areas (Bech et al., 2009; see Sect. 3.3 for further details).

Finally, all the information gathered needs to be organized and archived in an easily interpretable way to analyse the strong-convective wind event. In the following subsections, three final deliverables are proposed to achieve this objective: (i). A standardized damage survey summary, (ii). A geolocated information table, and (iii). A data location map. These deliverables are illustrated explicitly with an example of the 15 October 2018 Malgrat de Mar tornado case (see location in Fig. 1), provided as Supplementary material.

2.3.1 DAMAGE SURVEY SUMMARY

The summary of the damage survey should be an overview of the analysed event, including a brief description of the information gathered during the fieldwork and the main conclusions from the analysis of these data. The proposed deliverable is divided in seven parts.

1). General event information. It includes geographic and time data of the analysed meteorological phenomenon following current international standards for disaster reports losses (De Groeve et al., 2014), such as names and codes of country (ISO 3166-1 alpha-3 specification), regions or provinces (NUTS code) and municipalities (LAU code). This part also must contain the start and end date and time (in UTC) of the event and hazard classification according to the Integrated Research on Disaster Risk peril classification and hazard glossary (IRDR, 2014), including the family, the main event and the peril type.

2). Fieldwork information. It describes specific data about team members, including their affiliation and email address. Moreover, date and time of the visits, estimation of the fieldwork coverage over the total affected area and a brief description of difficult access areas should also be provided.

3). Initial sources of information. It contains information available (web pages and links) on media and social networks and developed funnel cloud images (if any), together with a brief explanation from the initial information gathered before starting the damage survey.

4). Meteorological conditions. This part describes weather conditions before, during and after the event according to direct witnesses, the visibility (darkness, precipitation), AWS data (location and a summary of the most relevant recorded data) and other data of interest derived from an overview of remote-sensing tools.

5) Damage observed. A general description of the observed damage is given (i.e. the most common and the most relevant seen during the fieldwork), including the maximum DoD for every DI noticed.

6). Direct witness inquiries. This part summarizes witness enquiries (which should also be attached apart). It should contain, if available, the duration of the strong winds and a brief description of the experience of each witness.

7). Characterization of the event. This final section contains the length and average and maximum width of the damage swath, the maximum wind intensity (specifying the intensity scale used), the translational direction and other data of interest such as the convective cell translation velocity.

2.3.2 GEOLOCATED DAMAGE TABLE

A geolocated information table providing disaggregated data for each point-of-damage is proposed, similarly as in Holzer et al. (2018). It should contain all relevant geolocated information gathered during the damage survey. To better organise the information displayed, seven different location types (L1 to L7, see Table 3) are considered. Note that L1 to L3 (vegetation and man-made structures) correspond to points-of-damage locations so that, if possible, they should include information about intensity rating (DI-DoD), according to Sect. 2.2. The rest of locations describe positions of AWS, witnesses, pictures or wind-borne debris.

2.3.3 DATA LOCATION MAP

The third deliverable consists of a map or a KML file format containing geolocated information gathered during the field survey in order to allow further graphical analysis, for example using Google Earth software (Gorelick et al., 2017). It is proposed that each of the seven location types presented in Sect. 2.3.2 are represented with a different icon, with a specific colour for points-of-damage (L1 to L3 from Table 3) depending on its intensity, which could be estimated using the EF-scale. Moreover, in case of damage in trees with fall direction (L1) it is convenient to display on the map an arrow icon, whose direction should be the fall direction. Thereby, a damage tree pattern analysis to discriminate between damage caused by a tornado or by a downburst should be easily carried out. Damage swath characteristics (length and width) should also be calculated using the data location map.

As an example, Fig. 7 shows the data location map of the fieldwork carried out on 25 March 2012 to study the EF1 tornado that affected the municipalities of Castellnou de Seana and Ivars d'Urgell (Catalonia) on 21 March 2012 (Bech et al., 2015). It displays the information contained in a fallen tree damage-point type (in this case, latitude, longitude, tree fall direction, DI-DoD, a brief description and a photo) and in the non-official Ivars d'Urgell AWS location (here, latitude, longitude, AWS type and maximum wind speed plot), which registered a maximum wind gust of 26.4 m s^{-1} during the event.

3 DISCUSSION

In this section, three main difficulties derived from the proposed methodology are discussed. Firstly, the geolocation accuracy, which affects directly some results such as the dimensions of the affected area (i.e. width and length of the damage swath); secondly, the uncertainty of damage intensity rating, mostly based on damage indicators developed in the USA if the EF-scale is employed; and, finally, the wind phenomenon type determination by a detailed analysis of forest damage patterns. Moreover, as already commented in Sect. 2, there are other limitations of the methodology such as getting information from difficult access sites or performing field surveys of very large areas.

3.1 GEOLOCATION ACCURACY

Geolocation accuracy of points-of-damage depends on a number of factors including local terrain geometry, quality of the receiver antenna system or number of satellites observed. Photo cameras and smartphones have location errors usually ranging from 5 to 20 meters, typically being greatest in deep valleys, or close to large buildings or structures blocking satellite signals. To minimize geolocation errors, it is recommended to check the accuracy with manually selected reference locations and, if necessary, to correct damage locations on the summary map and on the geolocated information table. This is feasible in urban or periurban areas, where buildings or other elements are easily identifiable using high-resolution aerial images such as ortophotos, but not in forests or other natural areas without evident references where this verification may not be possible.

3.2 DAMAGE INTENSITY RATING UNCERTAINTY

This subsection discusses briefly problems related with the application of an intensity scale not fully adapted to the region of study. Despite the proposed methodology is illustrated using the EF-scale for wind estimation, it should be noted that other intensity scales could be used such as the TORRO scale (Meaden et al., 2007).

The practical application of the EF-scale has some limitations (Doswell et al., 2009), in spite of the progress made some years ago by introducing a more detailed intensity-rating scale (WSEC, 2006) compared to the original and simpler Fujita scale (Fujita, 1981, 1992). The Enhanced Fujita scale, developed in the USA, is mainly based on the damage caused by wind on standard US buildings and elements (schools, hospitals, automobile showrooms, etc.), so-called Damage Indicators (DI). When applied to areas outside the USA many DI may not exist, hampering its application as discussed in detail Feuerstein et al. (2011)) and Holzer et al. (2018). Moreover, there are elements which are susceptible to being damaged such as traffic signals, walls and fences, trash bins and vehicles, which are not included on the EF-scale.

Possible solutions to this problem include considering specific studies reporting strong wind effects, for instance, on vehicles (Paulikas et al., 2016; Haan et al., 2017), proposals to introduce new DI to the EF-scale (Mahieu and Wesolek, 2016) or adapt them to typical man-made structures from other countries as recently reported in Canada (Environment Canada, 2013) or Japan (Japan Meteorological Agency, 2015). In any case, current progress in developing a standardized International Fujita Scale, as proposed in Groenemeijer et al. (2019), is an important step towards solving this issue.

3.3 TORNADO VS. DOWNBURST DAMAGE PATTERNS

The determination of the damaging wind phenomenon (tornado, downburst or straight line wind) can be rather challenging in some cases. As reported in previous studies (Hall and Brewer, 1959; Holland et al., 2006; Bech et al., 2009; Beck et al., 2010; Rhee and Lombardo, 2018), it can be assumed that the direction of fallen trees indicate the direction of maximum wind speed in strong-convective wind events, provided there are no influences from the terrain (i.e. slope favouring a specific fall direction) or from another tree fall interacting with the tree considered. Despite real damage wind patterns can be very complex, idealized damage swath patterns of both tornado and downburst wind fields can be compared with observed damage in order to look for similarities to assess their possible origin.

As explained in Bech et al. (2009), a simple approximation to describe a tornado vortex wind field near the surface is given by the Rankine vortex model, which combines an inner rigidly rotating core with an outer region with decreasing rotation speed. The wind field velocity module is defined in polar coordinates by Eq. (1):

$$v(r) = \begin{cases} \frac{v_{max} r}{R} & \text{if } r \leq R \\ \frac{v_{max} R}{r} & \text{if } r > R \end{cases} \quad (1)$$

where $v(r)$ is the wind velocity in function of the distance to the centre of the vortex r, v_{max} is the maximum wind velocity, and R is the vortex radius where $v(r) = v_{max}$.

Note that according to Eq. (1) the Rankine vortex can describe in simple terms only a rotating vortex and its nearby environment, i.e. a stationary vortex. To model real tornadoes, a Rankine vortex with both tangential and radial wind components is combined with a translational movement, i.e. a homogeneous wind field. As described in Bech et al. (2009), according to Peterson (1992), two parameters are used to characterize this model: parameter G, which is the ratio between tangential velocity and translational velocity, and parameter α, which is the angle between radial velocity and tangential velocity, corresponding 0° to a pure inflow, 90° to a pure tangential case and 180° to a pure outflow.

Examples of two-dimensional wind fields with different parameter configurations are shown in Fig. 8, including also their associated damage swath pattern shown as a rectangular panel below each two-dimensional wind field. The damage swath pattern is obtained computing the maximum wind vector of the wind field along the y axis, as the examples assume a northern translation of the vortex. In the first row (Fig. 8 a, b, and c panels), translational velocity is 1/4 tangential velocity ($G = 4$) and, in the second row (Fig. 8 d, e and f panels) translational velocity is equal to tangential velocity ($G = 1$).

In Fig. 8a, where tangential and inflow velocities are equal ($\alpha = 45°$), a convergence damage pattern is identified, whereas in Fig. 8b, where the radial component is zero ($\alpha = 90°$, i.e. pure tangential flow), the damage swath presents a rotational pattern. Fig. 8c presents pure outflow with no tangential velocity ($\alpha = 180°$), exhibiting a similar divergence pattern as Fig. 8f, in the damage swath, which could correspond with a classical downburst pattern.

Thus, based on this simple model, if fallen trees patterns present convergence or rotation, it can be assumed that a rotating vortex caused the damage, whereas a divergent pattern would suggest the effects of a downburst. Similarly, the way how debris is spread or how a roof is collapsed or lifted can indicate winds with either a rotation and upward pattern (i.e. a tornado), or with a divergent and downward pattern (i.e. a downburst) – see Rhee and Lombardo (2018) for a more detailed discussion.

Figure 9a shows a real example of fallen trees in a poplar plantation caused by the 15 October 2018 Malgrat de Mar tornado (see Supplementary material for more details). Figure 9b shows a plan view of the area showing with coloured arrows the direction of fallen trees. It can be seen that fallen trees follow a convergence pattern: in the right-half side from the damage swath, poplar trees are blown down to the west, whereas in the left-half side they are uprooted to the north. According to Fig. 8, this damage pattern can be associated with a vortex with $G = 4$ and $\alpha = 45°$ (Fig. 8a), which is also coherent with the damage rated as the lower EF1 bound and the mean translational velocity of 12 m s^{-1}, estimated using radar data from the Meteorological Service of Catalonia (not shown), as proposed in Sect. 2.3.

Nevertheless, it is also noticeable that in cases where tangential and translational velocities are similar ($G \approx 1$, see for example the second row of the Fig. 8), damage swaths may present only little differences among them. This can occur in weak (EF0 or EF1) tornado or downburst events that affect a small area, from which there are neither images nor direct witnesses. In these cases, damage also may be sparse, scattered and unconnected, which makes unidentifiable any damage pattern consistent with a tornado or a microburst (Bech et al., 2009; Rhee and Lombardo, 2018). Then, even a detailed damage survey may not be sufficient to determine which type of phenomena caused the damage. This situation of inconclusive results regarding the phenomenon type occurred in 7 % of the 136 damage surveys carried out in Spain by the authors from 2004 to 2018.

4 Summary and concluding remarks

Damage survey assessment data are used to study the consequences of natural hazards, which include floods or strong- convective damaging winds. Specifically the latter can be characterized carrying out field surveys, estimating damage path length and width, and also the intensity of the event. Moreover, they are also useful to clarify which phenomenon caused the damage (tornado, downburst or straight-line winds) in case neither images nor direct witness reports exist.

The purpose of the presented methodology is to provide a systematic and easily-reproducible methodology to carry out strong-convective wind event damage surveys, mainly based on gathering geolocated information about damaged man-made structures and vegetation, with the final aim of representing the damage scenario to study the event from a meteorological point of view. Complementary data from AWS close to the affected area and witness reports should be gathered if available. With all this information, three final deliverables are generated (a standardized summary of the fieldwork, a table consisting of detailed geolocated information, and a map or a file in KML format). The whole data set allows further analysis and archive purposes.

This methodology is based on previous studies and has been refined during the elaboration of 136 strong-convective wind damage surveys carried out in Spain between 2004 and 2018. Known limitations of its application include geolocation errors of damage, applicability of the EF-scale outside the USA and inconclusive determination of phenomenon type (tornado or downburst) in weak events, low visibility cases or low-density population affected areas. In any case, the field survey data obtained are valuable for further analysis, complementing meteorological detailed case studies based on operational remote sensing such as Doppler weather radar data, surface observations and Numerical Weather Prediction fields. Moreover, the methodology proposed may contribute to standardize detailed field surveys, which are essential to build up and maintain robust and homogeneous databases of severe weather phenomena.

Data availability. The data used in this paper is available from the authors upon request.

Competing interests. The authors declare that they have no conflict of interest.

Acknowledgements. The authors gratefully acknowledge individuals supporting wind damage assessments carried out during these years, especially to Joan Arús, Andrés Cotorruelo, Petra Ramos and particularly to Miquel Gayà for his pioneer systematic studies of tornadoes in Spain, and also the Consorcio de Compensación de Seguros (CCS) support. This research was performed with partial funding from projects CGL2015-65627-C3-2-R (MINECO/FEDER), CGL2016-81828-REDT (AEI) and RTI2018-098693-B643-C32 (AEI), and also from the Water Research Institute (IdRA) of the University of Barcelona.

References

Antonescu, B., Schultz, D. M., Holzer, A., and Groenemeijer, P.: Tornadoes in Europe: An underestimated threat, B. Am. Meteorol. Soc., 98, 713–728, https://doi.org/10.1175/BAMS-D-16-0171.1, 2017.

Antonescu, B., Schultz, D. M., Lomas, F., and Kühne, T.: Tornadoes in Europe: Synthesis of the observational datasets, Mon. Weather Rev., 144(7), 2445–2480, https://doi.org/10.1175/MWR-D-15-0298.1, 2016.

Bech, J., Arús, J., Castán, C., Pineda, N., Rigo, T., Montanyà, J., and van der Velde, O.: A study of the 21 March 2012 tornadic quasi linear convective system in Catalonia, Atmos. Res., 158–159, 192–209, https://doi.org/10.1016/j.atmosres.2014.08.009, 2015.

Bech, J., Gayà, M., Aran, M., Figuerola, F., Amaro, J., and Arús, J.: Tornado damage analysis of a forest area using site survey observations, radar data and a simple analytical vortex model, Atmos. Res., 93, 118–130, https://doi.org/10.1016/j.atmosres.2008.10.016, 2009.

Bech, J., Pascual, R., Rigo, T., Pineda, N., López, J. M., Arús, J., and Gayà, M.: An observational study of the 7 September 2005 Barcelona tornado outbreak, Nat. Hazards Earth Sys., 7, 129–139, https://doi.org/10.5194/nhess-7-129-2007, 2007.

Bech, J., Pineda, N., Rigo, T., and Aran, M.: Remote sensing analysis of a Mediterranean thundersnow and low-altitude heavy snowfall event, Atmos. Res., 123, 305–322, https://doi.org/10.1016/j.atmosres.2012.06.021, 2013.

Bech, J., Pineda, N., Rigo, T., Aran, M., Amaro, J., Gayà, M., Arús, J., Montanyà, J., and van der Velde, O.: A Mediterranean nocturnal heavy rainfall and tornadic event. Part I: Overview, damage survey and radar analysis, Atmos. Res., 100(4), 621–637, https://doi.org/10.1016/j.atmosres.2010.12.024, 2011.

Beck, V., and Dotzek, N.: Reconstruction of Near-Surface Tornado Wind Fields from Forest Damage. J. Appl. Meteorol. Climatol., 49, 1517–1537, https://doi.org/10.1175/2010JAMC2254.1, 2010.

Beven, K. J., Aspinall, W. P., Bates, P. D., Borgomeo, E., Goda, K., Hall, J. W., Page1, T., Phillips, J. C., Simpson, M., Smith, P. J., Wagener, T., and Watson, M.: Epistemic uncertainties and natural hazard risk assessment – Part 2: What should constitute good practice?, Nat. Hazards Earth Sys., 18, 2769–2783, https://doi.org/10.5194/nhess-18-2769-2018, 2018.

Bunting, W.F., and Smith, B.E.: A guide for conducting damage surveys. NOAA Tech. Memo. NWS-SR-146, Scientific Services Division, Southern Region, Fort Worth, TX, 44 pp., 1993.

Burgess, D., Ortega, K., Stumpf, G., Garfield, G., Kartens, C., Meyer, T., and Smith, B.: 20 May 2013 Moore, Oklahoma, Tornado: Damage Survey and Analysis, Weather Forecast., 29, 1229–1237, https://doi.org/10.1175/WAF-D-14-00039.1, 2014.

Chernokulsky, A., and Shikhov, A.: 1984 Ivanovo tornado outbreak: Determination of actual tornado tracks with satellite data, Atmos. Res., 207, 111–121, http://doi.org/10.1016/j.atmosres.2018.02.011, 2018.

De Groeve, T., Poljansek, K., and Ehrlich, D.: Recording disasters losses: recommendation for a European approach. JRC Scientific and Policy Report, available at: http://publications.jrc.ec.europa.eu/repository/bitstream/111111111/29296/1/lbna26111enn.pdf, last access: 2 December 2019, 2013.

De Groeve, T., Poljansek, K., Ehrlich D., and Corbane C.: Current status and best practices for disaster loss data recording in EU Member States. JRC Scientific and Policy Report, available at: http://publications.jrc.ec.europa.eu/repository/bitstream/JRC92290/lbna26879enn.pdf, last access: 2 December 2019, 2014.

Doswell III, C. A.: A guide to F-scale damage assessment, NOAA Rep., 101 pp., available at: www.wdtb.noaa.gov/courses/ef-scale/lesson2/FinalNWSF-scaleAssessmentGuide.pdf, 2003.

Doswell III, C. A., Brooks, H. E., and Dotzek, N.: On the implementation of the enhanced Fujita scale in the USA, Atmos. Res., 93, 554–563, https://doi.org/10.1016/j.atmosres.2008.11.003, 2009.

Dotzek, N., Groenemeijer, P., Feuerstein, B., and Holzer, A. M.: Overview of ESSL's severe convective storms research using the European Severe Weather Database ESWD, Atmos. Res., 93, 575–586, https://doi.org/10.1016/j.atmosres.2008.10.020, 2009.

Edwards, R., LaDue, J. G., Ferree, J. T., Scharfenberg, K., Maier, C., and Coulbourne, W. L.: Tornado Intensity Estimation: Past, Present, and Future, B. Am. Meteorol. Soc., 94, 641–653, https://doi.org/10.1175/BAMS-D-11-00006.1, 2013.

Environment Canada: Enhanced Fujita Scale Damage Indicators and Degrees Of Damage, available at: https://www.canada.ca/en/environment-climate-change/services/seasonal-weather-hazards/enhanced-fujita-scale-wind-damage.html, last access: 11 August 2019, 2013.

Farnell, C., Busto, M., Aran, M., Andrés, A., Pineda, N., and Torà, M.: Study of the hailstorm of 17 September 2007 at the Pla d'Urgell. Part one: fieldwork and analysis of hailpads, Tethys, 6, 67–79, https://doi.org/10.3369/tethys.2009.6.05, 2009.

Feuerstein, B., Groenemeijer, P., Dirksen, E., Hubrig, M., Holzer, A. M., and Dotzek, N.: Towards an improved wind speed scale and damage description adapted for Central Europe, Atmos. Res., 100, 547–564, https://doi.org/10.1016/j.atmosres.2010.12.026, 2011.

Foster, D. R.: Species and stand response to catastrophic wind in Central New England, U.S.A., J. Ecol., 76, 135–151, https://doi.org/10.2307/2260458, 1988.

Fujita, T. T.: Tornadoes and downbursts in the context of generalized planetary scales, J. Atmospheric Sci., 38(8), 1511–1534, https://doi.org/10.1175/1520-0469(1981)038<1511:TADITC>2.0.CO;2, 1981.

Fujita, T. T.: Mystery of severe storms. Wind Research Laboratory Research Paper 239, Dept. of Geophysical Sciences, University of Chicago, Chicago, IL, 298 pp, 1992. [NTIS PB-182021.]

Gayà, M.: Els Fiblons a Espanya: Climatologia i catàleg de tornados i trombes (Whirlwinds in Spain: Climatology and Catalog of Tornadoes and Waterspouts, in Catalan), Second edition, Edicions UIB, Palma, Spain, 619 pp., 2018.

Gayà, M., Llasat, M. C., and Arús, J.: Tornadoes and waterspouts in Catalonia (1950–2009), Nat. Hazards Earth Sys., 11(7), 1875-1883, https://doi.org/10.5194/nhess-11-1875-2011, 2011.

Godfrey, C. M., and Peterson, C. J.: Estimating Enhanced Fujita Scale Levels Based on Forest Damage Severity. Weather Forecast., 32: 243–252, https://doi.org/10.1175/WAF-D-16-0104.1, 2017.

Gorelick, N., Hancher, M., Dixon, M., Ilyushchenko, S., Thau, D., and Moore, R.: Google Earth Engine: Planetary-scale geospatial analysis for everyone, Remote Sens. Environ., 202, 18–27, https://doi.org/10.1016/j.rse.2017.06.031, 2017.

Groenemeijer, P., Holzer, A. M., Hubrig, M., Kühne, T., Kaltenberger, R., Soriano, J. D., Bock, L., Guitiérrez, D., van de Ploeg, B., Strommer, G., and Schreiner, T.: The International Fujita Scale: A Globally Applicable Scale for Tornado and Wind Damage Classification, 10th European Conference on Severe Storms, Kraków, Poland, 4–8 November 2019, 2019.

Gutiérrez, D., Riesco, J., and Ponce, S.: SINOBAS, a tool for collaborative mapping applied to observation of "singular" weather phenomena, 15th EMS Annual Meeting & 12th European Conference on Applications of Meteorology (ECAM), Sofia, Bulgaria, 7–11 September 2015, EMS2015-413, 2015.

Haan, F. L., Sarkar, P. P., Kopp, G. A., and Stedman, D. A.: Critical wind speeds for tornado-induced vehicle movements, J. Wind. Eng. Ind. Aerodyn., 168, 1–8, https://doi.org/10.1016/j.jweia.2017.04.014, 2017.

Hall, F., and Brewer, R. D.: A sequence of tornado damage patterns, Mon. Weather Rev., 87, 207–216, 1959.

Holland, A. P., Riordan, A. J., and Franklin, E. C.: A simple model for simulating tornado damage in forests, J. Appl. Meteorol. Climatol., 45, 1597–1611, https://doi.org/10.1175/JAM2413.1, 2006.

Holzer, A. M., Schreiner, T. M. E., and Púčik, T.: A forensic re-analysis of one of the deadliest European tornadoes, Nat. Hazards Earth Syst. Sci., 18, 1555–1565, https://doi.org/10.5194/nhess-18-1555-2018, 2018.

Hyvärinen, O., and Saltikoff, E.: Social Media as a Source of Meteorological Observations. Mon. Weather Rev., 138, 3175–3184, https://doi.org/10.1175/2010MWR3270.1, 2010.

IRDR: Peril Classification and Hazard Glossary, Integrated Research on Disaster Risk, 28 pp., available at: http://www.irdrinternational.org/2014/03/28/irdr-peril-classification-and-hazard-glossary/, last access: 27 December 2019, 2014.

Japan Meteorological Agency (JMA): Guidelines for the Japanese Enhanced Fujita Scale, 113 pp., available at: https://www.data.jma.go.jp/obd/stats/data/bosai/tornado/kaisetsu/jefscale_en.html, last access: 11 August 2019, 2015.

Karstens, C. D., Samaras, T. M., Lee, B. D., Gallus, W. A., and Finley, C. A.: Near-Ground Pressure and Wind Measurements in Tornadoes. Mon. Weather Rev., 138, 2570–2588, https://doi.org/10.1175/2010MWR3201.1, 2010.

Karstens, C. D., Gallus, W. A., Lee, B. D., and Finley, C. A.: Analysis of Tornado-Induced Tree Fall Using Aerial Photography from the Joplin, Missouri, and Tuscaloosa–Birmingham, Alabama, Tornadoes of 2011, J. Appl. Meteorol. Climatol., 52, 1049–1068, https://doi.org/10.1175/JAMC-D-12-0206.1, 2013.

Knox, J. A., Rackley, J. A., Black, A. W., Gensini, V. A., Butler, M., Dunn, C., Gallo, T., Hunter, M. R., Lindsey, L., Phan, M., Scroggs, R., and Brustad, S.: Tornado Debris Characteristics And Trajectories During The 27 April 2011 Super Outbreak As Determined Using Social Media Data, B. Am. Meteorol. Soc., 94, 1371–1380, https://doi.org/10.1175/BAMS-D-12-00036.1, 2013.

Kryvasheyeu, Y., Chen, H., Obradovich, N., Moro, E., Van Hentenryck, P., Fowler, J., and Cebrian M.: Rapid assessment of disaster damage using social media activity, Sci. Adv., 3(2), e1500779, http://doi.org/10.1126/sciadv.1500779, 2016.

Letchford, C. W., and Chay, M. T.: Pressure distributions on a cube in a simulated thunderstorm downburst. Part B: moving downburst observations, J. Wind. Eng. Ind. Aerodyn., 90, 733–753, https://doi.org/10.1016/S0167-6105(02)00163-0, 2002.

Li, L., Yang, J., Lin, C.-Y., Chua, C. T., Wang, Y., Zhao, K., Wu, Y.-T., Liu, P. L.-F., Switzer, A. D., Mok, K. M., Wang, P., and Peng, D.: Field survey of Typhoon Hato (2017) and a comparison with storm surge modeling in Macau, Nat. Hazards Earth Syst. Sci., 18, 3167–3178, https://doi.org/10.5194/nhess-18-3167-2018, 2018.

Llasat, M. C., Turco, M., Quintana-Seguí, P., and Llasat-Botija, M.: The snow storm of 8 March 2010 in Catalonia (Spain): a paradigmatic wet-snow event with a high societal impact, Nat. Hazards Earth Sys., 14(2), 427, http://www.doi.org/10.5194/nhess-14-427-2014, 2014.

Mahieu, P., and Wesolek, E.: Tornado Rating in Europe with the EF-scale, KERAUNOS, 65 pp., available at: http://www.keraunos.org/tornado-rating-in-europe-with-the-enhanced-fujita-scale.pdf, last access: 11 August 2019, 2016.

Marshall, T. P.: Tornado damage survey at Moore, Oklahoma. Weather Forecast., 17, 582–598, https://doi.org/10.1175/1520-0434(2002)017<0582:TDSAMO>2.0.CO;2, 2002.

Marshall, T., Davis, W., and Runnels, S.: Damage survey of the Joplin tornado, 26th Conference on Severe Local Storm, Nashville, TN, USA, 5–8 November 2012, 6.1, available at: https://ams.confex.com/ams/26SLS/webprogram/Manuscript/Paper211662/Joplinmerger.pdf, last access: 11 August 2019, 2012.

Mateo, J., Ballart, D., Brucet, C., Aran, M., and Bech, J.: A study of a heavy rainfall event and a tornado outbreak during the passage of a squall line over Catalonia, Atmos. Res., 93(1–3), 131–146, https://doi.org/10.1016/j.atmosres.2008.09.030, 2009.

Matsangouras, I. T., Nastos, P. T., Bluestein, H. B., and Sioutas, M. V.: A climatology of tornadic activity over Greece based on historical records, Int. J. Climatol., 34(8), 2538–2555, https://doi.org/10.1002/joc.3857, 2014.

Meaden, G. T., Kochev, S., Kolendowicz, L., Kosa-Kiss, A., Marcinoniene, I., Sioutas, M., Tooming, H., and Tyrrell, J.: Comparing the theoretical versions of the Beaufort scale, the T-Scale and the Fujita scale, Atmos. Res., 83(2–4), 446–449, https://doi.org/10.1016/j.atmosres.2005.11.014, 2007.

Meng, Z., and Yao, D.: Damage Survey, Radar, and Environment Analyses on the First-Ever Documented Tornado in Beijing during the Heavy Rainfall Event of 21 July 2012, Weather Forecast., 29, 702–724, https://doi.org/10.1175/WAF-D-13-00052.1, 2014.

Miglietta, M. M., and Matsangouras, I. T.: An updated “climatology” of tornadoes and waterspouts in Italy, Int. J. Climatol., 38(9), 3667–3683, https://doi.org/10.1002/joc.5526, 2018.

Miller, P. W., and Mote, T. L.: Characterizing severe weather potential in synoptically weakly forced thunderstorm environments, Nat. Hazards Earth Sys., 18(4), 1261–1277, https://doi.org/10.5194/nhess-18-1261-2018, 2018.

Molinari, D., Menoni, S., Aronica, G. T., Ballio, F., Berni, N., Pandolfo, C., and Minucci, G.: Ex post damage assessment: an Italian experience, Nat. Hazards Earth Sys., 14: 901–916, http://doi.org/10.5194/nhess-14-901-2014, 2014.

Paulikas, M. J., Schmidlin, T. W., and Marshall, T. P.: The Stability of Passenger Vehicles at Tornado Wind Intensities of the (Enhanced) Fujita Scale, Weather Clim. Soc., 8, 85–91, https://doi.org/10.1175/WCAS-D-15-0051.1, 2016.

Peterson, R. E.: Johannes Letzmann: a pioneer in the study of tornadoes, Weather Forecast. 7 (1), 166–184, https://doi.org/10.1175/1520-0434(1992)007<0166:JLAPIT>2.0.CO;2, 1992.

Renko, T., Ivušić, S., Prtenjak, M. T., Šoljan, V., and Horvat, I.: Waterspout forecasting method over the eastern Adriatic using a high-resolution numerical weather model, Pure Appl. Geophys., 175 (11), 3759–3778, https://doi.org/10.1007/s00024-018-1833-x, 2018.

Rhee, D. M., and Lombardo, F. T.: Improved near-surface wind speed characterization using damage patterns, J. Wind. Eng. Ind. Aerodyn., 180, 288–297, https://doi.org/10.1016/j.jweia.2018.07.017, 2018.

Riesco, J., Polvorinos, F., Núñez, J. A., Soriano, J. D., and Jiménez, C.: Climatología de tornados en España Peninsular y Baleares (Tornado Climatology in the Peninsular Spain and Balearic Islands, in Spanish), Spanish Meteorological Agency (AEMet), 83 pp., available at: http://www.aemet.es/documentos/es/conocermas/publicaciones/Climatologia_tornados/Climatologia_tornados.pdf, last access: 11 August 2019, 2015.

Ripoll, R., del Amo, X., and Vendrell, R.: The weather observers network of the Meteorological Service of Catalonia, WMO Technical Conference on Meteorological and Environmental Instruments and Methods of Observation (CIMO TECO 2016), Madrid, Spain, 27–30 September 2016, P2(57), 2016.

Rodríguez, O., and Bech, J.: Sounding-derived parameters associated with tornadic storms in Catalonia, Int. J. Climatol., 38, 2400–2414, http://doi.org/10.1002/joc.5343, 2018.

Roueche, D. B., and Prevatt, D. O.: Residential Damage Patterns Following the 2011 Tuscaloosa, AL and Joplin, MO Tornadoes, J. Disaster Res, 8(6), 1061–1067, 2013.

Sánchez-Laulhé, J. M.: El tornado de Málaga del 1 de Febrero de 2009 (The 1 February 2009 tornado of Malaga, in Spanish), Spanish Meteorological Agency (AEMet), 3 pp., available at: https://repositorio.aemet.es/bitstream/20.500.11765/2724/1/TyC_2009_24_03.pdf, last access: 11 August 2019, 2013.

Shikhov, A., and Chernokulsky, A.: A satellite-derived climatology of unreported tornadoes in forested regions of northeast Europe, Remote Sens. Environ., 204, 553–567, https://doi.org/10.1016/j.rse.2017.10.002, 2018.

Shikhov, A. N., Perminova, E. S., Perminov, S. I.: Satellite-based analysis of the spatial patterns of fire-and storm-related forest disturbances in the Ural region, Russia, Nat. Hazards, 1–26, https://doi.org/10.1007/s11069-019-03642-z, 2019.

Strader, S. M., Ashley, W., Irizarry, A., and Hall, S.: A climatology of tornado intensity assessments, Meteorol. Appl., 22, 513–524, https://doi.org/10.1002/met.1482, 2015.

Taszarek, M., Brooks, H. E., and Czernecki, B.: Sounding-Derived Parameters Associated with Convective Hazards in Europe, Mon. Weather Rev., 145, 1511–1528, https://doi.org/10.1175/MWR-D-16-0384.1, 2017.

Verbout, S. M., Brooks, H. E., Leslie, L. M., and Schultz, D. M.: Evolution of the US tornado database: 1954–2003, Weather Forecast., 21(1), 86–93, https://doi.org/10.1175/WAF910.1, 2006.

WSEC: A Recommendation for an Enhanced Fujita Scale (EF-scale), Wind Science and Engineering Center, 111 pp., available at: http://www.spc.noaa.gov/faq/tornado/EFScale.pdf, last access: 11 August 2019, 2006.

Wakimoto, R. M., Wienhoff, Z., Bluestein, H. B., and Reif, D.: The Dodge City Tornadoes on 24 May 2016: Damage Survey, Photogrammetric Analysis Combined with Mobile Polarimetric Radar Data, Mon. Weather Rev., 146(11), 3735–3771, https://doi.org/10.1175/MWR-D-18-0125.1, 2018.

Wurman, J., Kosiba, K., and Robinson, P.: In situ, Doppler radar, and video observations of the interior structure of a tornado and the wind–damage relationship, B. Am. Meteorol. Soc., 94(6), 835–846, https://doi.org/10.1175/BAMS-D-12-00114.1, 2013.

Zanini, M. A., Hofer, L., Faleschini, F., and Pellegrino, C.: Building damage assessment after the Riviera del Brenta tornado, northeast Italy. Nat. Hazards, 86, 1247–1273, http://doi.org/10.1007/s11069-017-2741-6, 2017.

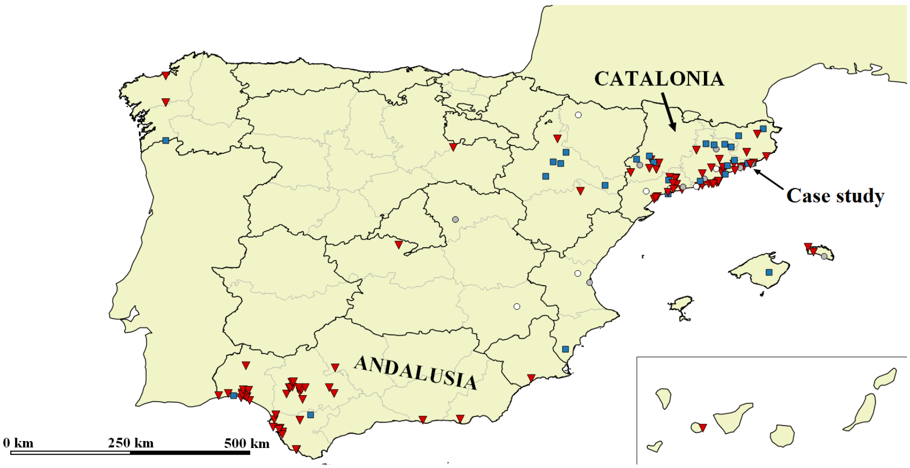

Figure 1. Location of 136 analysed events using the proposed methodology between 2004 and 2018, mostly concentrated in Andalusia and Catalonia. Symbols indicate locations of tornadoes (red triangles), downbursts (blue squares), undetermined phenomena (grey circles) and other phenomena such as gust fronts, funnel clouds which did not touch down, or dust devils (white circles). The case study location for which final deliverables are attached as Supplementary material is indicated on the map.

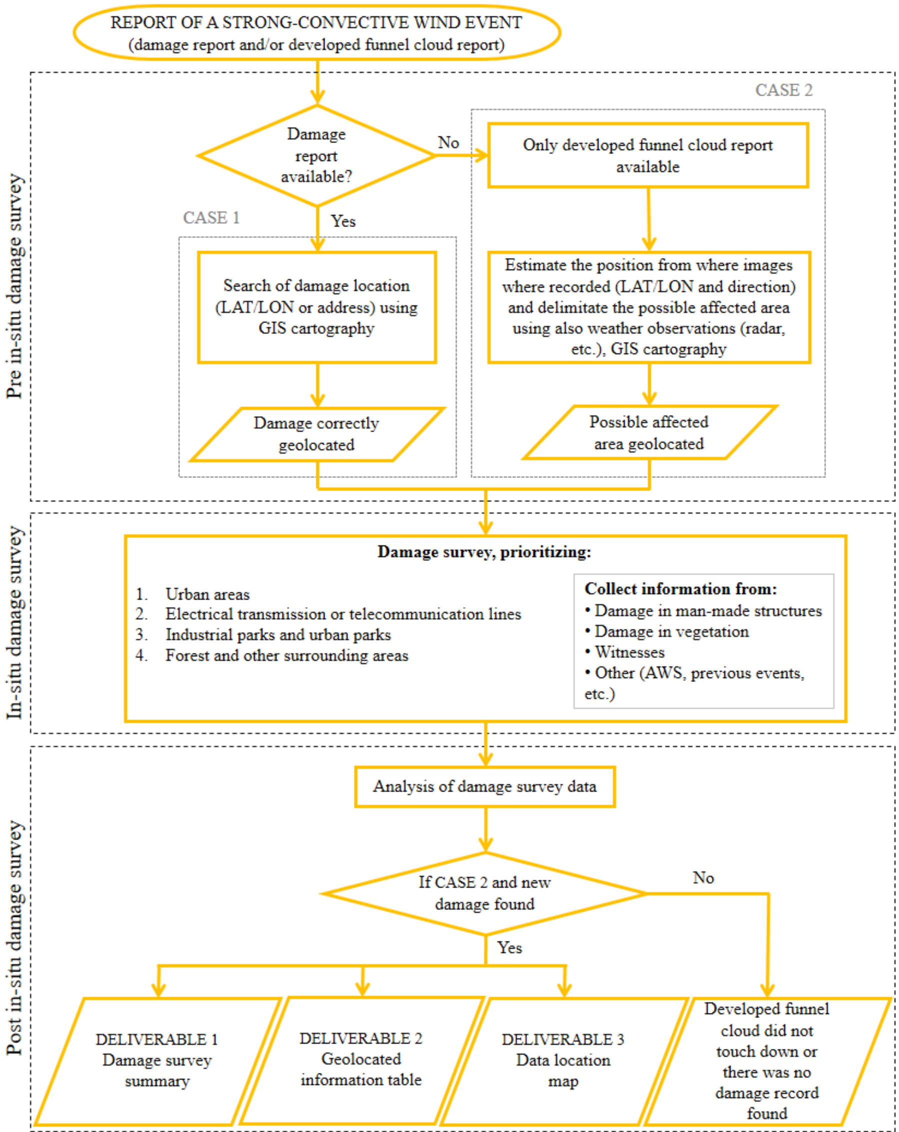

Figure 2. Flow diagram of the structure and application of the proposed methodology to carry out strong-convective winds fieldwork damage assessment.

Figure 3. Clearing service of Zaragoza (Aragón, NE Spain) removing broken branches after the 11 July 2018 downburst (Author: Salvador Castán)

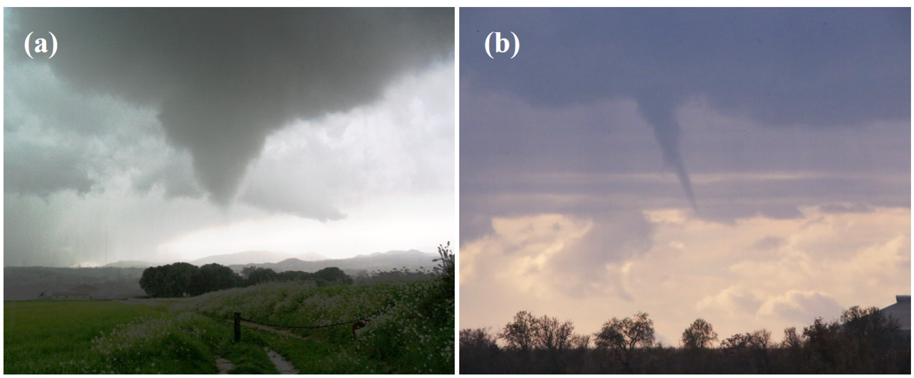

Figure 4. (a) Developed funnel cloud observed in Santa Eulàlia de Ronçana (Catalonia) on 4 April 2010 (Author: @CalabobosChaser). (b) Developed funnel cloud observed in Bellpuig (Catalonia) on 1 December 2017 (Author: Edgar Aldana). In both cases no evident tornado was actually observed (i.e. touchdown) but nearby damage was reported suggesting tornado occurrence.

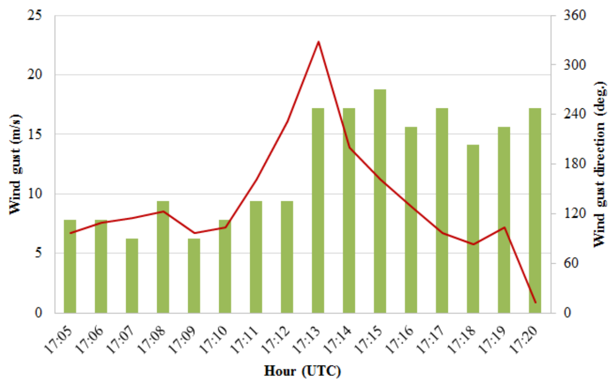

Figure 5. Wind gust (red line) and wind gust direction (green bars) registered by an AWS in Mataró (Catalonia) with 1 minute resolution data. The AWS was located 240 m west of the estimated centre of the EF0 tornado track, on 23 November 2016. Data source: Meteomar, Consell Comarcal del Maresme.

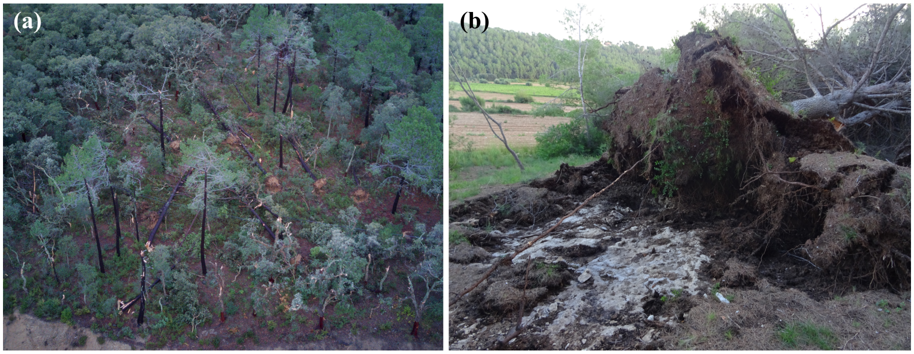

Figure 6. (a) Drone image of a mixed Mediterranean forest in Darnius (NE Catalonia) where most pine trees were blown down whereas cork oaks were only slightly affected with broken branches by an EF2 tornado, on 7 January 2018 (Author: Jonathan Carvajal). (b) Pine blown down by an EF0 tornado in Perafort (Catalonia) in a very thin, moist soil area, on 14 October 2018 (Author: Oriol Rodríguez).

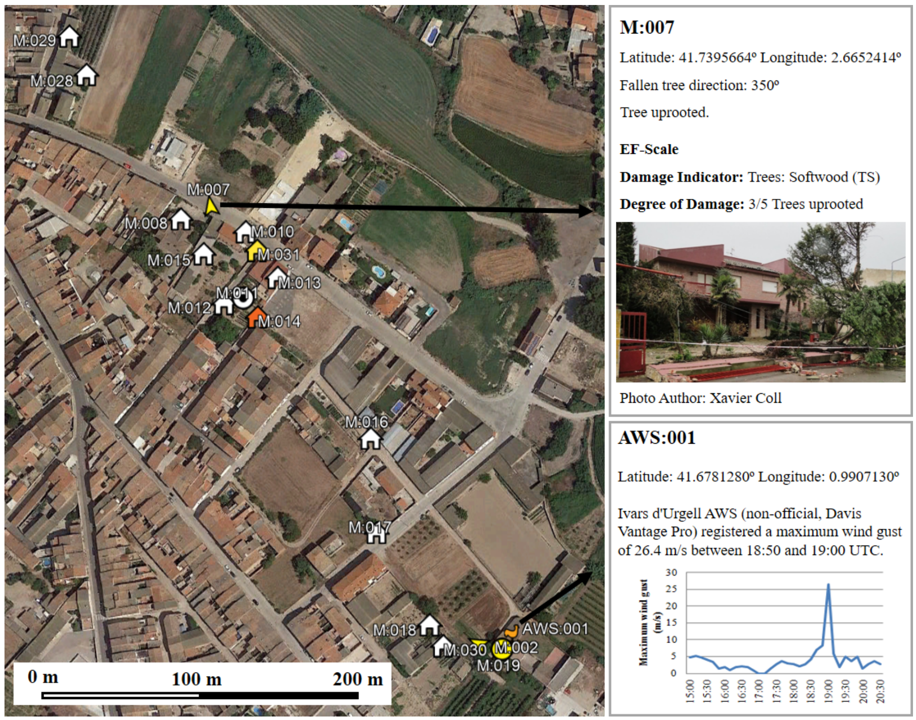

Figure 7. Data location map and two examples of recorded information from the 21 March 2012 EF1 Ivars d'Urgell (Catalonia) tornado track. Map symbols indicate locations of AWS (orange weather vane), damage in man-made structures (house icons) and fallen tree or damaged vegetation element (arrow and circle icons if no direction is available, respectively). Icon colours indicate damage intensity using the EF-scale: EF0 (yellow), EF1 (orange), and unrated (white). The background ortophoto is from the Institut Cartogràfic i Geològic de Catalunya (ICGC), http://www.icc.cat/ (last access: September 2019), under a CC BY 4.0 license.

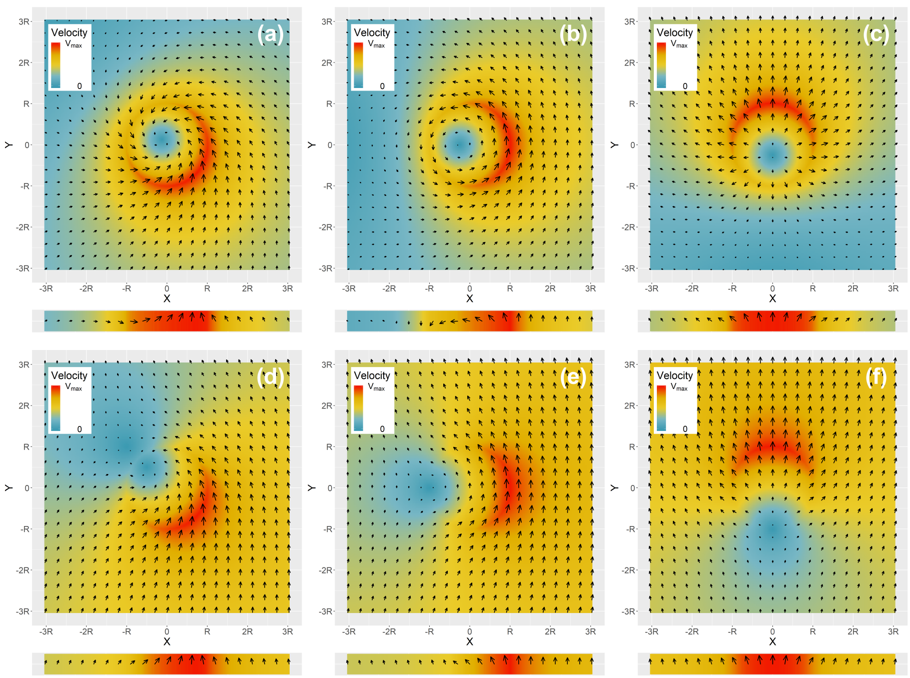

Figure 8. Two dimensional near surface horizontal wind fields and damage swaths for the cases (a) $G = 4$ and $\alpha = 45°$, (b) $G = 4$ and $\alpha = 90°$, (c) $G = 4$ and $\alpha = 180°$, (d) $G = 1$ and α =45°, (e) $G = 1$ and $\alpha = 90°$, and (f) $G = 1$ and $\alpha = 180°$. Adapted from Figures 3 and 4 of Bech et al. (2009)

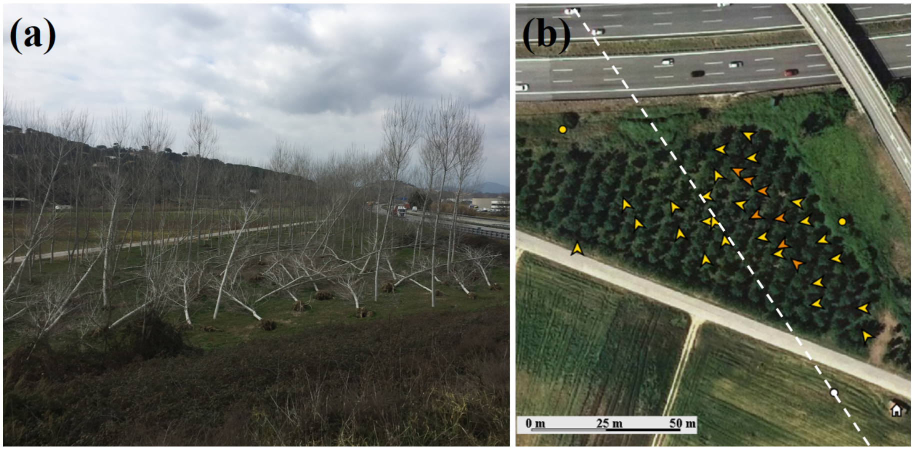

Figure 9. (a) A poplar plantation from Fogars de la Selva (Catalonia) affected by the EF1 Malgrat de Mar - Massanes tornado, on 15 October 2018, and (b) fallen trees directions of the same poplar plantation. Map symbols indicate locations of damage in man-made structures (house icons) and fallen tree or damaged vegetation element (arrow or circle icons if no direction is available). Icon colours indicate damage intensity: EF0 (yellow), EF1 (orange), and unrated (white). The white discontinuous line separates the right-half and the left-half sides of the damage swath where predominant fall tree direction are west and north, respectively. The background ortophoto is from the Institut Cartogràfic i Geològic de Catalunya (ICGC), http://www.icc.cat/ (last access: September 2019), under a CC BY 4.0 license.

Table 1. Variables and typical uncertainties of data descriptors for damaged man-made structures and vegetation elements. The first four variables are required for all damaged elements (both man-made structures and vegetation). Degraded state or previous weakness of damaged elements should also be reported. Dragged distance, direction and weight of wind-borne debris should be measured. Fallen tree direction and trunk diameter should be measured in case of uprooted and snapped trees, respectively.

Variable	Uncertainty	Comment
Latitude	$\pm 1 \cdot 10^{-4}$ deg.	Measured with GPS camera.
Latitude	$\pm 1 \cdot 10^{-4}$ deg.	Measured with GPS camera.
Damage Indicator (DI)	—	Determined during the post in-situ damage survey using intensity-rating scales as EF-scale.
Degree of Damage (DoD)	—	Determined during the post in-situ damage survey using intensity-rating scales as EF-scale.
Previous weakness	—	Description of deficiencies that can increase the vulnerability of elements to strong winds.
Dragged distance object	± 1 m	Distance between the final position and the origin of an object displaced by the wind. Measured with a tape measure or GIS tools.
Dragged direction object	± 5 deg.	Direction of the displacement. Measured with a compass or GIS tools.
Weight of wind-borne debris	< 10 %	Weight of an object of interest moved by the wind. In case of small objects, measured with a balance if possible.
Fallen tree direction	± 5 deg.	In case of uprooted trees. Measured with a compass.
Trunk diameter	± 5 cm	In case of snapped trees. The trunk perimeter is measured with a tape measure and then the diameter can be calculated.

Table 2. Witness enquiry questions (reference and question).

Question reference	Question
Q1	At what time did the phenomenon occur?
Q2	Where were you when the phenomenon took place?
Q3	How long did the strongest winds last? (Some seconds, around one minute, several minutes…).
Q4	During the phenomenon, did you hear any special or rare noise?
Q5	How was the weather like before, during and after the phenomenon? (Light rain, heavy rain, small hail, large hail, snow, no precipitation).
Q6	Have you noticed other areas with damage?
Q7	Do you remember any similar phenomenon in this area before?

Table 3. Information location types (reference, description and data that should be presented).

Location reference	Description	Data
L1	Damage in trees with fall direction	Latitude, longitude, DI-DoD, previous weaknesses, fall direction
L2	Damage in trees without fall direction	Latitude, longitude, DI-DoD, previous weaknesses, trunk diameter (if snapped tree)
L3	Damage in man-made structures	Latitude, longitude, DI-DoD, previous weaknesses
L4	AWS location	Latitude, longitude, data (maximum wind gust, direction of maximum wind gust and hour)
L5	Witness location	Latitude, longitude of the witness location at the moment of the meteorological event and a brief description of his experience
L6	Image of the phenomenon	Latitude, longitude from the point where image was recorded and orientation
L7	Wind-borne debris	Latitude, longitude, distance and direction of the displacement, size and weight of the object if measured